

In the Classroom

Chemical Oscillations in Enzyme Kinetics

KATHERINE L. QUEENEY¹, ETHAN P. MARIN¹,
CORY M. CAMPBELL², and ENRIQUE PEACOCK-LÓPEZ^{3,*}

¹ Department of Chemistry, Williams College, Williamstown, MA 01267

² Department of Anesthesiology, San Diego Veteran Administration
Medical Center, 3350 La Jolla Village Drive, San Diego, CA 92161

³ Institute of Theoretical Dynamics, University of California,
Davis, CA 95616

*The Higgins
model is a two
variable model in
enzyme kinetics
... [which] shows
steady states,
damped
oscillations and
stable limit
cycles.*

The Higgins model is a two variable model in enzyme kinetics. In contrast with other popular simple dynamical models like the Lotka–Volterra model, the Higgins model shows steady states, damped oscillations and stable limit cycles. For these three dynamical behaviors, stability analysis yields expressions of the eigenvalues, which are easy to obtain either analytically or with the use of Mathematica. With these expressions we can find the boundaries between the three dynamical regions in parameter space and the bifurcation point. Also, we have compared the Higgins model with the other two variable models and find that the origin of the richer dynamical behavior of the Higgins model is due to the enzymatic step in the mechanism.

* Permanent address: Department of Chemistry, Williams College, Williamstown, MA 01267

Introduction

For the last thirty years sustained oscillations in the concentration of a chemical substance have been the subject of intensive study. In spite of theoretical predictions of damped oscillations and sustained oscillations by Lotka and Hirniakand [1, 2] in 1910 and Lotka [3] in 1920, and the experimental observation of cyclic changes in the iodate catalyzed decomposition of hydrogen peroxide by Bray in 1921 [4], both experimentalists and theorists virtually ignored the field of chemical oscillations for nearly thirty years. Finally, in the early 1950s Belusov [5, 6] observed cyclic color changes in the bromination of citric acid catalyzed by cerium. By 1967 the first paper on the Belusov–Zhabotinsky (B–Z) [7] reaction written in English reached the West. This reaction caused immense interest among so many researchers that the First Symposium on Biological and Biochemical Oscillators was organized in 1968, forty seven years after Bray’s paper appeared in the *Journal of the American Chemical Society*.

An interesting aspect of the B–Z system centers around the original motivation that led Belusov to the celebrated reaction. Originally, his interest in biochemistry, and in particular in the Krebs cycle [8], motivated Belusov to seek a simple experimental model in which a carbohydrate was oxidized in the presence of a catalyst. In other words, the B–Z reaction was intended as a model of an enzyme catalyzed reaction. This connection between enzyme kinetics and the B–Z reaction is often forgotten and rarely mentioned. Most likely, this omission can be traced to the differences between an enzyme and its model counterpart Ce, the complicated mechanism underlining the chemical oscillations in the B–Z reaction and the mathematical analyses needed to understand some of the reduced models of the B–Z reaction. From the biochemical point of view these differences are difficult to reconcile with a biological model; therefore, the search for a model of chemical oscillation in enzyme kinetics that is both biochemically relevant and mathematically simple enough to present to an undergraduate audience is worthwhile from the pedagogical point of view.

In the present discussion we consider glycolysis emphasizing the allosteric properties of phosphofructokinase (PFK). For nearly thirty years oscillations in the concentration of nucleotides in the glycolytic pathway have been documented in the case of yeast cells and cell-free extract [9]. For example, reduced nicotinadenine dinucleotide (NADH) oscillations in yeast extract have been observed and determined to be flux dependent, and a minimum external flux is required to sustain oscillations in the concentration of NADH. Moreover, Hess and Boiteux [10] observed that phosphofructokinase plays an

essential role in these oscillations. If PFK's substrate, fructose-6-phosphate (F-6-P), is added to cell-free extracts, the nucleotide concentrations oscillate. On the other hand, after the injection of PFK's product, fructose-1,6-bisphosphate (F-1,6-bP), no oscillations are observed. Based on these observations and on the allosteric properties of PFK, two models were suggested in the late 1960s. One, by Higgins [11], is based on the activation of PFK by its product. The second model by Sel'kov [12] is based on the activation and inhibition properties of PFK by ATP, ADP, and AMP. The latter links PFK with pyruvate kinase, while the former does not.

In the next section we discuss the steps along the glycolytic pathway that are relevant to the Higgins model. Next, we reduce the model to two variables and discuss its similarities with Lotka's models and the origin of the autocatalytic step. Finally, we scale the model, do a linear stability analysis, and discuss the bifurcation diagram of the reduced, two-variable Higgins model.

Higgins Model

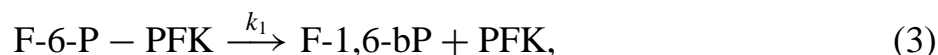
The interest in the origin of periodic biological processes like the circadian clock has motivated researchers to look for the chemical basis of oscillations in biochemical systems [13–15]. One of these systems is glycolysis, in which six-membered sugars are converted anaerobically into tricarboxylic acids and ADP gets phosphorylated. In the case of glycolysis the addition of glucose to an extract containing the main metabolites triggers cyclic, or periodic, behavior in the concentrations of metabolites. These periodic changes in the concentrations of the glycolytic metabolites are termed glycolytic relaxation oscillations. In particular, relaxation oscillations in the concentration of NADH are readily observed using spectrophotometric methods on yeast extracts. For the past thirty years researchers have mostly studied relaxation oscillations that are due to a single injection of glucose. In this case the system relaxes to equilibrium. Conversely, if constant or periodic injection is applied, a system is pushed away from equilibrium and can achieve nonequilibrium steady states.

Researchers have found that phosphofructokinase, which catalyzes the conversion of F-6-P to F-1,6-bP, is the regulatory enzyme for glycolytic oscillations [16–17]. This regulation is the result of the activation and inhibition properties of PFK. For example, in liver PFK is activated by F-2,6-bP [18], which is an isomer of F-1,6-bP. In muscle PFK is inhibited by ATP. Based on these facts, most kinetic models of glycolytic oscillations have centered

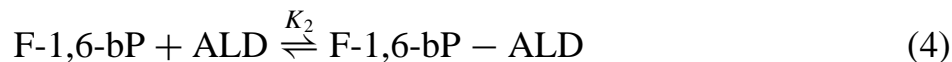
around either PFK's inhibition [12] or its activation [11]. One of the models, based on the activation of PFK by fructose biphosphate, is the Higgins model. This model considers only two enzymatic reactions with a constant external source of glucose. Condensing two steps of the glycolytic path into one, the Higgins model assumes a first order conversion of glucose to F-6-P.



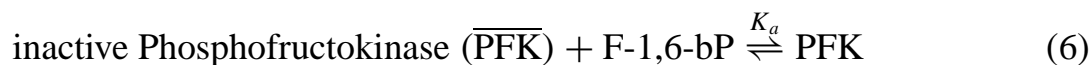
Following this first step, the Higgins model considers the enzymatic conversion of F-6-P to F-1,6-bP by PFK



and F-1,6-bP to glyceraldehyde-3-phosphate by aldolase (ALD).



In this model the regulation consists only of the activation of PFK by F-1,6-bP.



Under this assumption the Higgins model sustains oscillations in the concentration of F-6-P, F-1,6-P, and the enzymes. Using further simplifications, such as the steady-state approximation for PFK, the model reduces to three time-dependent species with autocatalytic conversion of F-6-P to F-1,6-bP. Finally, if one considers a steady-state approximation for ALD, one obtains a two-species model that is able to sustain oscillations.

For the sake of a simple notation, the following mechanism, which is equivalent to equations 1–6, will be used.





where G stands for glucose, X for F-6-P, E_1 for PFK, Y for F-1,6-bP and E_2 for ALD. Using these equations, the mass action laws for the six species model are as follows:

$$\frac{d[X]}{dt} = k_o G_o - k_{E_1}^+ [E_1][X] + k_{E_1}^- [E_1 X] \quad (16)$$

$$\frac{d[Y]}{dt} = k_1 [E_1 X] - k_{E_2}^+ [E_2][Y] + k_{E_2}^- [E_2 Y] - k_a^+ [\bar{E}_1][Y] + k_a^- [E_1] \quad (17)$$

$$\frac{d[E_1]}{dt} = k_{E_1}^- [E_1 X] - k_{E_1}^+ [E_1][X] + k_1 [E_1 X] - k_a^- [E_1] + k_a^+ [\bar{E}_1][Y] \quad (18)$$

$$\frac{d[E_1 X]}{dt} = -k_{E_1}^- [E_1 X] + k_{E_1}^+ [E_1][X] - k_1 [E_1 X] \quad (19)$$

$$\frac{d[\bar{E}_1]}{dt} = k_a^- [E_1] - k_a^+ [\bar{E}_1][Y] \quad (20)$$

$$\frac{d[E_2]}{dt} = k_{E_2}^- [E_2 Y] - k_{E_2}^+ [E_2][Y] + k_2 [E_2 Y] = -\frac{d[E_2 Y]}{dt} \quad (21)$$

Using the steady-state approximation for all of the enzymes, we obtain a minimal two variable model

$$\frac{d[X]}{dt} = k_o G_o - k_{ac} [X][Y] \quad (22)$$

$$\frac{d[Y]}{dt} = k_{ac}[X][Y] - \frac{V_{2m} \frac{[Y]}{K_{2M}}}{1 + \frac{[Y]}{K_{2M}}}, \quad (23)$$

where k_{ac} is given by the following equation:

$$k_{ac} = \frac{K_a \frac{V_{1m}}{K_{1M}}}{1 + K_a[Y] + \frac{K_a}{K_{1M}}[X][Y]} \quad (24)$$

and

$$K_{iM} = \frac{k_i + k_{E_i}^-}{k_{E_i}^+} \quad (25)$$

$$V_{im} = k_i E_i^\circ \quad (26)$$

$$K_a = \frac{k_a^+}{k_a^-} \quad (27)$$

In equation 26 E_i° represents the stoichiometric concentration of the i^{th} enzyme. Also, in the Higgins model, k_{ac} is simplified even further [19] to

$$k_{ac} = \frac{V_{1m} K_a}{K_{1M}} = \frac{k_1 k_{E_1}^+ E_i^\circ K_a}{k_1 + k_{E_1}^-} \quad (28)$$

Equations 22–28 constitute the Minimal Higgins (MH) model.

The Minimal Higgins Model as expressed by equations 22 and 23 shows some similarities with the Lotka models. The two Lotka models are the simplest schemata in which oscillations in the populations can be observed. A meaningful interpretation of the Lotka model is in population dynamics. For example, if we define G as grass, R as rabbit, and W as wolf, the explanation of the oscillatory behavior seems quite logical. As the rabbits consume the grass and reproduce, their numbers grow. As the rabbit population grows, the wolves have plenty of rabbits available for consumption, and they, too, reproduce. As the wolf population increases, however, the rabbit population decreases. As the rabbit population decreases, the wolves start to die, because there are not enough rabbits. As a consequence the rabbits start the cycle again. For example, in the original Lotka model of 1910 species reproduction is proportional to the amount of food, which is kept constant;

namely



This elementary step, in conjunction with the following steps:



define what is known as the Lotka Model and the differential equations describing the time behavior of the population are given in Table 1. Notice that the first differential equations in the MH model and in Lotka's 1910 model are the same.

In the 1920 paper, Lotka introduces a species dependent external flux; namely



which is an autocatalytic step and substitutes for equation 29. As in the previous case, the amount of grass, G_o , is kept constant; the differential equations associated with this model are given in Table 1. Notice that the 1920 model, also known as the Lotka–Volterra model [20], is a variation of the 1910 model in which the external flux is modified from a zeroth-order process to an autocatalytic first-order process. Consequently, we can think of the MH model as a variation of the 1910 Lotka model, where we have included an enzymatic step instead of a first order process in equation 31.

Unfortunately, the first Lotka model yields only damped oscillations, and the Lotka–Volterra model yields neutrally stable cycles for any initial conditions [21–23], which is a severe restriction if we want to model realistic chemical and biochemical system. In contrast, the Minimal Higgins model shows stable steady states and stable oscillations usually called limit cycles. The richness of this model stems from the second differential equation, which includes an enzymatic Michaelis-Menten step. Moreover, the autocatalytic step in the MH model can be linked to the activation of PFK by its product.

For completeness, we have included a fourth model in Table 1. This model is due to Schnakemberg [24] and is related to the Sel'kov model. In this model the bimolecular autocatalytic step in the Lotka 1910 model is replaced by a trimolecular step. This

TABLE 1. Two variable models and their associated differential equations.

Model	Differential equations
Lotka 1910	$\frac{d[R]}{dt} = k_R G_o - k_W [R][W]$ $\frac{d[W]}{dt} = k_w [R][W] - k_D [W]$
Lotka 1920	$\frac{d[R]}{dt} = k_R G_o [R] - k_W [R][W]$
Lotka–Volterra	$\frac{d[W]}{dt} = k_w [R][W] - k_D [W]$
Minimal Higgins	$\frac{d[X]}{dt} = k_o G_o - k_{ac} [X][Y]$ $\frac{d[Y]}{dt} = k_{ac} [X][Y] - \frac{V_{2m} [Y]}{K_{2M} + [Y]}$
Schnakenberg	$\frac{d[X]}{dt} = k_o G_o - k_S [X][Y]^2$ $\frac{d[Y]}{dt} = k_S [X][Y]^2 - k_D [Y]$

change appears as a cubic term in the differential equations. With this change, the model shows stable oscillations, but the connection between the cubic autocatalytic term and a biochemical justification has not been achieved.

Linear Stability Analysis

In this section we present a linear stability analysis [21–23] of the Minimal Higgins model. For this purpose, we scale the differential equation such that the dimensionless differential equations depend only on two parameters rather than on five. Namely, we get

from equations 22 and 23

$$\frac{dX}{d\tau} = A - XY \equiv f_1(X, Y) \quad (33)$$

$$\frac{dY}{d\tau} = XY - \frac{qY}{1+Y} \equiv f_2(X, Y) \quad (34)$$

where we have defined the following dimensionless quantities

$$\tau = k_{ac} K_{2M} t \quad (35)$$

$$X = \frac{[X]}{K_{2M}} \quad (36)$$

$$Y = \frac{[Y]}{K_{2M}} \quad (37)$$

$$A = \frac{k_o G_o}{K_{2M}^2 k_{ac}} \quad (38)$$

$$q = \frac{V_{2m}}{K_{2M}^2 k_{ac}} \quad (39)$$

The first step in the stability analysis is to find the steady state solution. In general this is done by setting the left hand side of the differential equations equal to zero and solving for the concentrations. From equations 33 and 34, we obtain, for the scaled MH model, the following steady state solutions

$$x^{ss} = q - A \quad (40)$$

$$y^{ss} = \frac{A}{q - A} \quad (41)$$

Clearly from equations 40 and 41, we see that only values of A less than q give meaningful solutions; i.e., x^{ss} and y^{ss} have to be positive. Physically this condition means that the maximum enzymatic rate, V_{2m} , has to be greater than the input flux, $k_o G_o$.

Once these stationary states are obtained, stability analysis studies what happens to all components of the system when it is perturbed slightly from its steady state. For this purpose we first calculate the relaxation matrix, R , which is the Jacobian associated with

a set of ordinary differential equations (ODEs) [21]

$$R = \begin{bmatrix} \left(\frac{\partial f_1}{\partial X}\right)_{(x^{ss}, y^{ss})} & \left(\frac{\partial f_1}{\partial Y}\right)_{(x^{ss}, y^{ss})} \\ \left(\frac{\partial f_2}{\partial X}\right)_{(x^{ss}, y^{ss})} & \left(\frac{\partial f_2}{\partial Y}\right)_{(x^{ss}, y^{ss})} \end{bmatrix} \quad (42)$$

For the scaled MH model, we obtain the following matrix.

$$R = \begin{bmatrix} -y^{ss} & -x^{ss} \\ y^{ss} & x^{ss} - \frac{q}{(1+y^{ss})^2} \end{bmatrix} \quad (43)$$

Next, we have to find the eigenvalues, λ_{\pm} , of R . In other words we have to find the solutions of the following equation.

$$|R - \lambda I| = 0 \quad (44)$$

where I is the two by two identity matrix. For the MH model, equation (44) reduces to the following characteristic polynomial.

$$\lambda^2 + \left(\frac{(1 + y^{ss})(y^{ss} - x^{ss}) + x^{ss}}{1 + y^{ss}}\right) \lambda + \left(\frac{x^{ss} y^{ss}}{1 + y^{ss}}\right) = 0 \quad (45)$$

Furthermore the solutions of the quadratic equation (45) are

$$\begin{aligned} \lambda_{\pm} = & -\frac{1}{2} \left(\frac{(1 + y^{ss})(y^{ss} - x^{ss}) + x^{ss}}{1 + y^{ss}}\right) \\ & \pm \frac{1}{2} \sqrt{\left(\frac{(1 + y^{ss})(y^{ss} - x^{ss}) + x^{ss}}{1 + y^{ss}}\right)^2 - 4 \left(\frac{x^{ss} y^{ss}}{1 + y^{ss}}\right)} \end{aligned} \quad (46)$$

Using equations 40 and 41, equation 46 can be reduced to the following expression

$$\lambda_{\pm} = \frac{P_R(A, q) \pm \sqrt{P_I(A, q)}}{2q(q - A)} \quad (47)$$

where we have defined the following functions.

$$P_R(A, q) = A [A^2 - 2Aq + q^2 - q] \quad (48)$$

$$P_I(A, q) = A \left[A^5 - 4qA^4 + 2q(3q + 1)A^3 - 4q^2(q + 2)A^2 + q^2(q^2 + 10q + 1)A - 4q^2 \right] \quad (49)$$

Equations (48) and (49) have been obtained both by analytical methods and with the help of the software package Mathematica [25].

Discussion

In this section we extract the information contained in equations 47–49, which were obtained in the previous section using linear stability analysis.

First, from equation 47, we can consider four possible sets of conditions: (a) In the case of $P_R < 0$ and $P_I > 0$, the eigenvalues are pure, real, and negative; thus, the steady state solution is a stable fixed point [21]; (b) when $P_R < 0$ and $P_I < 0$ the eigenvalues have a negative real part and a nonzero imaginary part; therefore these eigenvalues give damped oscillations; (c) for $P_R > 0$ and $P_I > 0$ the eigenvalues are pure, real, and positive; therefore, the steady state is unstable; and (d) if $P_R > 0$ and $P_I < 0$, the eigenvalues have a positive real part and a nonzero imaginary part; thus, the steady state is unstable, and the state of the system tends to move away from the steady state and approaches stable oscillations.

Second, using equations 48 and 49, we can construct a plot of A vs. q , where we can easily observe different regions, each corresponding to different dynamical behaviors. Figure 1 depicts such a diagram, and the different lines represent curves where $A - q$, P_I , and P_R are equal to zero; these curves delimit different regions in parameter space. In region A, $P_I > 0$ and $P_R < 0$; thus, we should observe stable fixed points. In region B, $P_I < 0$ and $P_R < 0$; therefore, we should observe damped oscillations. Finally, in region C, $P_I < 0$ and $P_R > 0$ and we should observe limit cycles.

Also, for a fixed value of q , the value of A at which $P_R(A, q)$ is equal to zero, A_c , defines the bifurcation point. From equation 48 the nontrivial solution to $P_R(A_c, q) = 0$, for a fixed value of q , is given by

$$A_c = q - \sqrt{q} \quad (50)$$

where we have used the physical condition $A < q$. Consequently, values of A greater than A_c are in regions A or B, and for values less than A_c are in region C. Thus for $A_c < A < q$

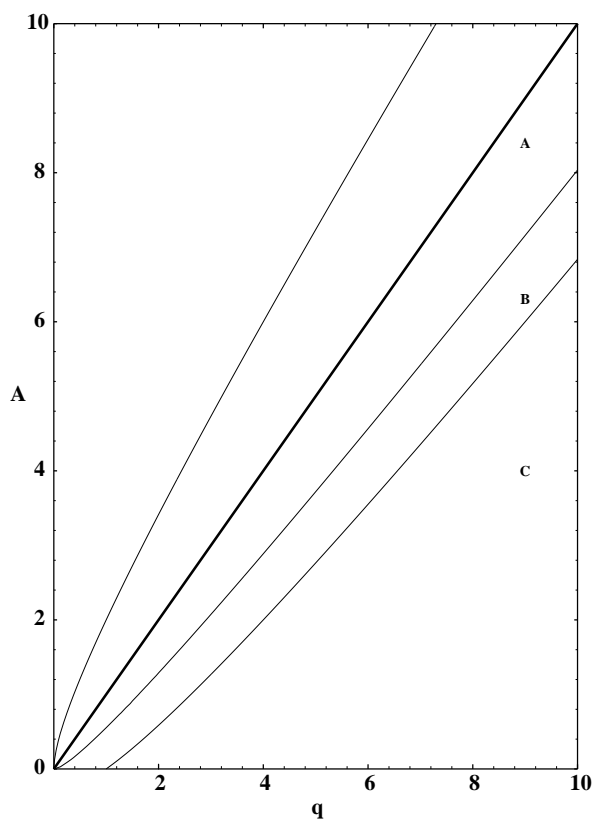


FIGURE 1. PARAMETER SPACE DIAGRAM FOR THE MINIMAL HIGGINS MODEL. REGION A IS LIMITED BY THE LINE $q = A$ AND $P_I(A, q) = 0$; REGION B IS LIMITED BY $P_I(A, q) = 0$ AND $P_R(A, q) = 0$; REGION C IS DEFINED BY $P_R(A, q) > 0$.

the system reaches a stable steady state. For $A < A_c$, the system reaches a limit cycle. As an example, if we consider $q = 10$, the bifurcation will occur at $A_c = 6.837$. With this information we can select different values of the dimensionless external flux, A , in such a way that different dynamical behaviors can be observed if we numerically integrate equations 33 and 34.

Finally, using Mathematica, we numerically integrate equations 33 and 34, with initial conditions $x(0) = 10$ and $y(0) = 10$, and generate Figures 2–4. First, we consider $q = 10$ and $A = 8.50$. These values represent a point in region A. Figure 2a depicts the approach of x to its steady state value ($x^{ss} = 1.5$), and Figure 2b shows the approach to the fixed point (1.5, 5.66) in xy phase space. Next, we consider $A = 6.87$. Figure 3a illustrates the time series of a damped oscillation as x approaches its steady state value of $x^{ss} = 3.13$. In Figure 3b, we observe in xy phase space the spiral in approach to the steady state ($x^{ss} = 3.13$, $y^{ss} = 2.19$). Finally, we consider $A = 6.5$. This value is less

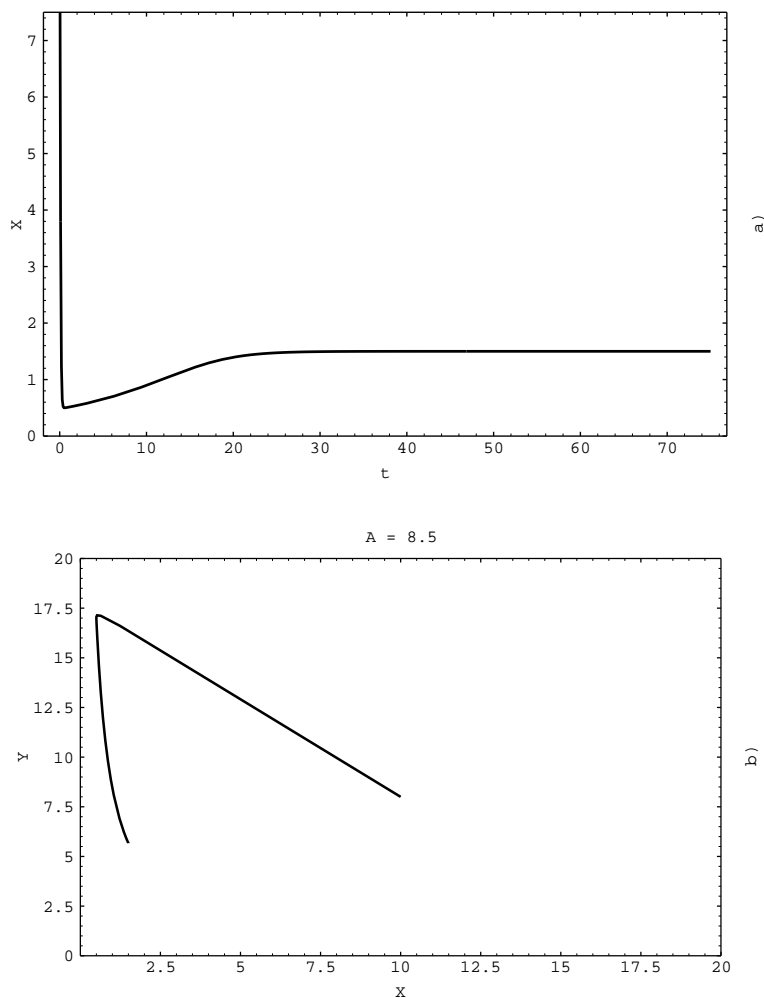


FIGURE 2. EXAMPLE OF A FIXED POINT. IN THIS CASE WE CONSIDER $q = 10$ AND $A = 8.50$, WHICH REPRESENTS A POINT IN REGION A. FIGURE (a) SHOWS THE TIME SERIES OF x WITH INITIAL VALUES $x = 10$ AND $y = 10$; FIGURE (b) DEPICTS THE BEHAVIOR IN xy PHASE SPACE.

than A_c , which means that stable oscillations could be observed. Figure 4a depicts the stable oscillations of x as a function of scaled time; Figure 4b shows the approach to a stable limit cycle around the unstable steady state ($x^{ss} = 3.5$, $y^{ss} = 1.86$).

The only problem associated with the MH model and inherent in all of the models in Table 1 is a fixed point at $y = 0$ and an infinitely large value of x . Numerically, for fixed q , the problem appears for small values of A . In some cases, Mathematica is not able to handle the numerical integrations and other algorithms are required to study the differential equations for small values of A [26, 27]. Modifications intended to remove

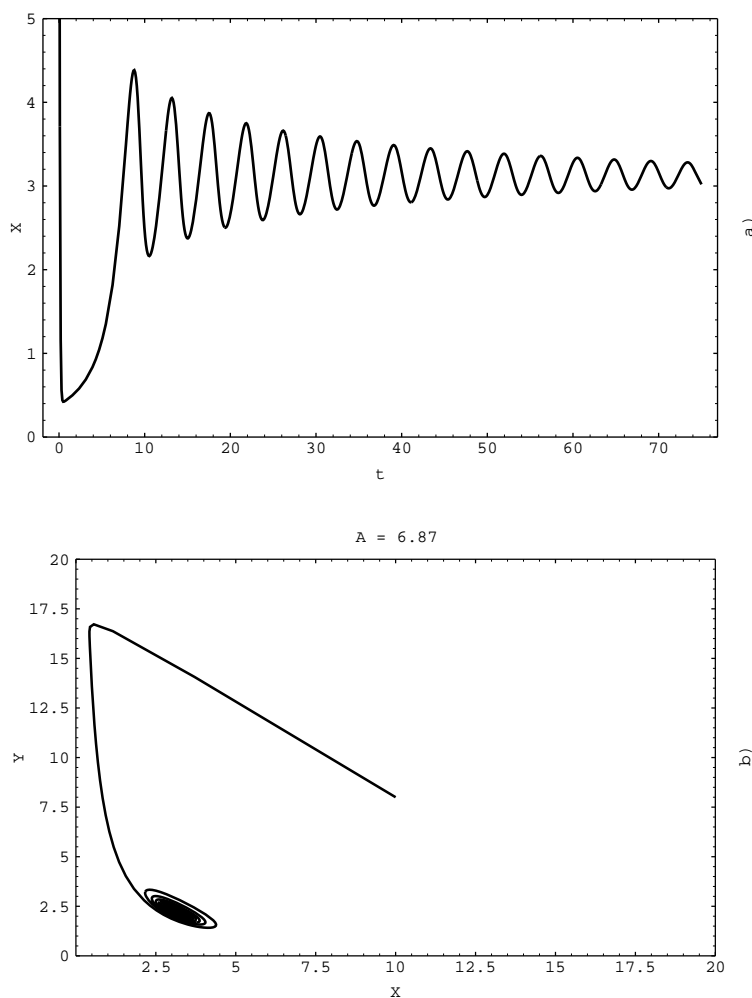


FIGURE 3. EXAMPLE OF DAMPED OSCILLATIONS. IN THIS CASE WE CONSIDER $q = 10$ AND $A = 6.87$, WHICH REPRESENTS A POINT IN REGION B. FIGURE (a) DEPICTS THE DAMPED OSCILLATIONS OF x AS A FUNCTION OF DIMENSIONLESS TIME WITH THE SAME INITIAL CONDITIONS AS IN FIGURE 2; FIGURE (b) DEPICTS THE SPIRAL IN APPROACH TO THE STABLE STEADY STATE IN x - y PHASE SPACE.

these kind of fixed points have been done to the Schnakenberg model. For example, the addition of a first order conversion of x into y is discussed in references [28–30].

Summary

The minimal Higgins model is a simple two-species model that shows stable steady states and limit cycles in enzyme kinetics. The steps in the mechanism have a biochemical justification and the step responsible for the stable oscillation is a Michaelis–Menten step. Furthermore, linear stability analysis of this model is simple and accessible both analytically or with the help of Mathematica; for example the bifurcation points are

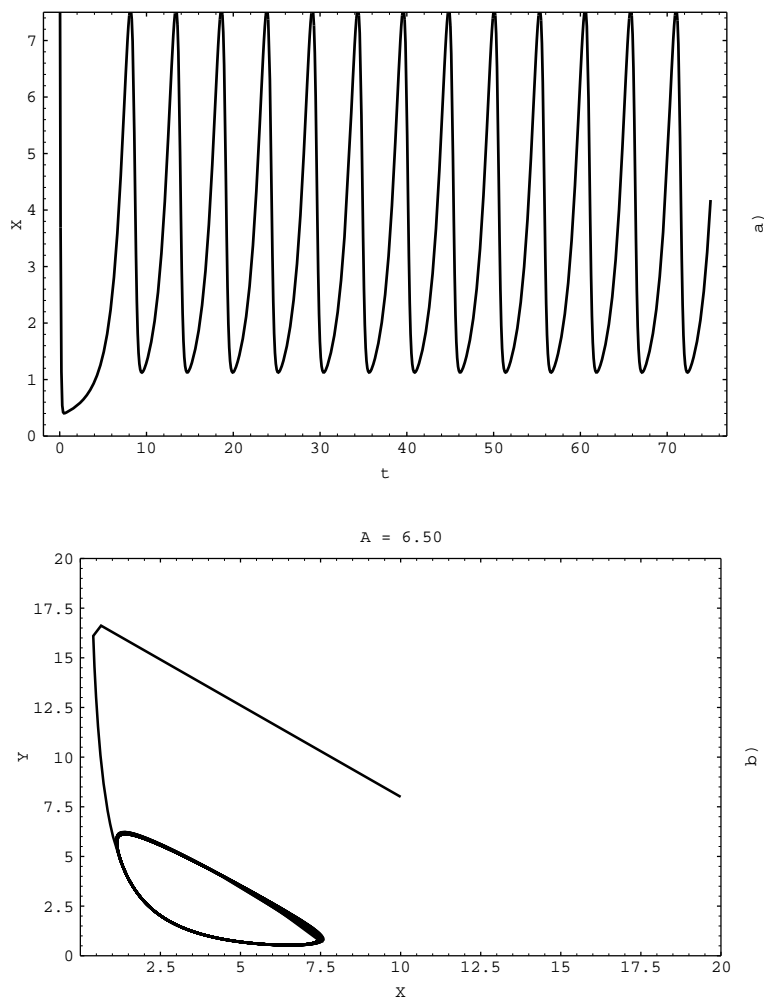


FIGURE 4. EXAMPLE OF A STABLE LIMIT CYCLE. IN THIS CASE WE CONSIDER $q = 10$ AND $A = 6.50$, WHICH REPRESENTS A POINT IN REGION C. FIGURE (a) DEPICTS THE STABLE OSCILLATIONS IN X AS A FUNCTION OF DIMENSIONLESS TIME WITH THE SAME INITIAL CONDITION AS IN FIGURE 2; FIGURE (b) SHOWS THE APPROACH TO THE LIMIT CYCLE IN XY PHASE SPACE.

obtained by fixing either A or q and solving a simple quadratic equation; that is, equation 50. Also, numerical integration of equations 33 and 34 both confirms and exemplifies the results obtained from linear stability analysis.

Acknowledgments

The authors would like to thank Casey H. Londergan for helpful comments. Also, support from the National Science Foundation (CHE 8915945 and CHE 9312160) is gratefully acknowledged. One of us (EP-L) has been partially supported by an NSF Research Opportunity Award during his sabbatical leave at the University of California Davis.

REFERENCES

1. Lotka, A. J. *J. Am. Chem. Soc.* **1910**, *42*, 1595.
2. Hirniak, Z. *Z. Physik. Chem.* **1910**, 675.
3. Lotka, A. J. *J. Phys. Chem.* **1920**, *14*, 271.
4. Bray, W. C. *J. Amer. Chem. Soc.* **1921**, *43*, 1262.
5. Belusov, B. P. *Sb. Ref. Radiats. Med. za 1958.* **1959**, *1*, 145.
6. Winfree, A. T. *J. Chem. Educ.* **1984**, *61*, 661.
7. Zhabotinsky, A. M. *Biofizika* **1964**, *9*, 306. (in Russian).
8. van Holde, M. *Biochemistry*; Benjamin: Redwood, 1990.
9. Gosh, A.; Chance, B. *Biochem. Biophys. Res. Commun.* **1964**, *16*, 174.
10. Boiteux, A.; Hess, B.; Sel'kov E. E. *Current Topics in Cellular Regulation* **1975**, *17*, 171.
11. Higgins, J. *Proc. Nat. Acad. Sci. U.S.* **1964**, *52*, 989.
12. Sel'kov, E. E. *Europ. J. Biochem.* **1968**, *4*, 79.
13. Banks, H. T. *Modeling and Control in the Biomedical Sciences*; Springer: Berlin, 1975.
14. Palmer, J. D. *An Introduction to Biological Rhythms*; Academic: New York, 1976.
15. Berridge, M. J.; Rapp, P. E.; Treherne, J. E. Eds. *Cellular Oscillators*; Cambridge: Cambridge, 1979.
16. Tornhein, K. *J. Theo. Biol.* **1979**, *79*, 491.
17. Tornhein, K. *J. Biol. Chem.* **1988**, *263*, 2619.
18. Pilkins, S. J.; Granner, D. K. *Annu. Rev. Physiol.* **1992**, *54*, 885.
19. Ibañez, J. L.; Fairém; and Velarde, M. G. *Phys. Lett.* **1976**, *58A*, 364.
20. Volterra, V. *Mem. Acad. Lincei.*, **1926**, *2*, 31.
21. Edelstein-Keshet, L. *Mathematical Models in Biology*; Random: New York, 1988.

22. Murray, J. D. *Mathematical Biology*; Springer: Berlin, 1993.
23. Strogatz, S. H. *Nonlinear Dynamics and Chaos*, Addison Wesley: Reading, 1994.
24. Schnakenberg, J. *J. Theo. Biol.* **1979**, *81*, 389.
25. Wolfram, S. *Mathematica, Ver. 2.1*; Wolfram Research, 1991.
26. Kahaner, D. K.; Barnett, D. D. *Plotted Solutions of Differential Equations (PLOD), Ver. 6.00*; NIST, Washington, DC. 1989.
27. Parker, T. S.; Chua, L. O. *Practical Numerical Algorithms for Chaotic Systems*; Springer: New York, 1989.
28. Gray, P.; Scott, S. K. *Chemical Oscillations and Instabilities*; Oxford: Oxford, 1990.
29. Scott, S. K. *Chemical Chaos*; Oxford: Oxford, 1993.
30. Peng, B.; Scott; S. K.; Showalter, K. *J. Phys. Chem.* **1990**, *94*, 5243.